

## Magnetic field behavior of $\text{Bi}_2\text{Sr}_2\text{CaCu}_2\text{O}_{8+\delta}$ Intrinsic Josephson Junctions

### $\text{Bi}_2\text{Sr}_2\text{CaCu}_2\text{O}_{8+\delta}$ Intrinsic 조셉슨 접합의 자기장 효과

J. H. Lee, H. J. Lee, Y. Chong, S. Lee, and Z. G. Khim

이주형, 이현주, 정연욱, 이수연, 김정구

Department of Physics, Seoul National University, Seoul 151-742

서울시 관악구 신림동 서울대학교 물리학과, 151-742

We have measured I-V characteristics of  $\text{Bi}_2\text{Sr}_2\text{CaCu}_2\text{O}_{8+\delta}$  mesa containing a small number of intrinsic stacked Josephson junctions in a magnetic field. We fabricated mesa with an area of  $40 \times 40 \mu\text{m}^2$  containing 3~20 intrinsic junctions. We applied magnetic field perpendicular to the  $\text{CuO}_2$  planes up to 5T. We observed flux-flow branches and flux-flow steps in the I-V characteristics which might be due to collective motion of Josephson vortices in the long junction limit. In a parallel field, critical current  $I_c$  varies as  $I_c(B) \sim \exp(-B/B_0)$ , where  $B_0$  is about 2T, which is consistent with the theoretical model. DC and AC intrinsic Josephson effects are also discussed.

### 1. Introduction

The highly anisotropic layered high- $T_c$  superconductor, such as  $\text{Bi}_2\text{Sr}_2\text{CaCu}_2\text{O}_8$  (BSCCO), exhibits the intrinsic Josephson effect. The Josephson tunneling occurs between superconducting  $\text{CuO}_2$  layers of thickness 3 Å separated by non-superconducting BiO and SrO layers of thickness 12 Å. This feature makes it possible to form a natural crystalline tunnel junction and to measure the inherent superconducting characteristics of the inter-layer tunneling [1,2].

Recently, c-axis tunneling measurements of small size mesa structure of BSCCO single crystals have been widely carried out. Also their behaviors in a high magnetic field have received increasing attentions [3,4].

The field-dependent tunneling characteristics provide information on the dynamics of

Josephson vortices and the interaction of pancake vortices via interlayer Josephson coupling which originates from parallel and perpendicular magnetic field to  $\text{CuO}_2$  planes respectively.

Dynamics of Josephson vortices are an important subject because of their electronic application to high frequency oscillator and high speed digital devices [5].

### 2. Experimental

The BSCCO single crystals were used to fabricate the mesa pattern. The crystal size was typically  $2 \text{ mm} \times 3 \text{ mm} \times 100 \mu\text{m}$  and it was glued on a Si substrate using stycast-1266. To protect the surface of BSCCO from contamination during the photolithography process, a 30 nm-thick Au layer was deposited using e-beam evaporator after *in-situ*

cleaving of the top surface. The mesa with lateral size of  $20 \times 20 \mu\text{m}^2$  and  $40 \times 40 \mu\text{m}^2$  were patterned using a standard photolithography and Ar ion beam etching technique.

Positive Az1512 Photoresist(PR) was used to fabricate stacks and negative Az5214 PR was used as the insulating material above which 500 nm-thick Au contact pads were deposited.

The fabricated mesa contains 1 ~ 30 intrinsic Josephson junctions whose number was controlled by the ion beam etching time. The mesa height was inferred from I-V measurement and from AFM image, and the results agreed well within 1 nm.

Four contacts were prepared with silver paste. The contact resistance ranges from 1 to 5  $\Omega$ . Figure 1 shows schematic diagram of the sample of BSCCO intrinsic junction.

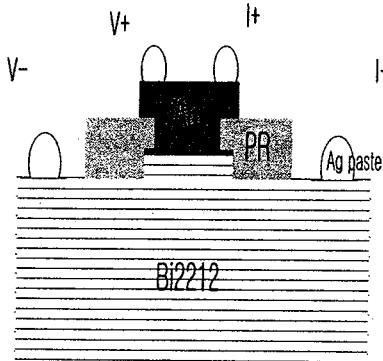


**FIG. 1.** Schematic diagram of stack fabricated on BSCCO single crystal.

The typical size of stack is  $40 \times 40 \times 0.01 \mu\text{m}^3$

The sample was loaded to MPMS Quantum Design SQUID magnetometer. We could vary temperature from 300 K to 4.2 K and magnetic field from 0 to 5.5 T.

To obtain I-V curves, a triangular shape current bias was applied at frequency less than 1 Hz and the resulting voltage difference across the junction was detected with a low noise pre-amplifier which was connected to a digital oscilloscope. As the current increases,

the voltage jumps from the zero voltage state to the first resistive state(first branch), the next branch(second branch) and so on. So multiple branches of I-V curves can be obtained by drawing all I-V curves with different current sweeps together.

### 3.Result and discussion

#### 3-1. Superconducting state , zero field I-V characteristics

Before measuring I-V characteristics, we measured the resistivity along the c-axis  $\rho_c$  as a function of temperature.

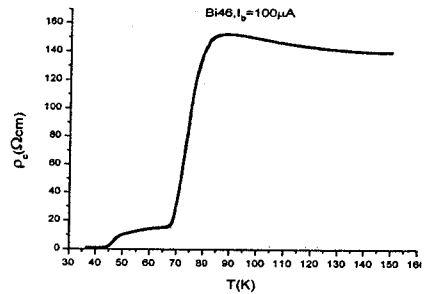


**FIG. 2.** Temperature dependence of c-axis resistivity of single intrinsic Josephson junction(IJJ). The Bias current is  $100 \mu\text{A}$ .

Fig. 2 is the result of the R-T measurement of the single intrinsic junction. It exhibits semiconducting temperature dependence. The bias current is rather high ( $100 \mu\text{A}$ ), so the transition region is broad and we can observe the tail of a typical Josephson junction as shown in the figure. At 150 K,  $\rho_c$  is  $140 \Omega\text{cm}$ , which is larger than the values reported in other studies[6]. And as the number of junctions increases, the semi-conducting feature is more prominently manifested above  $T_c$ .

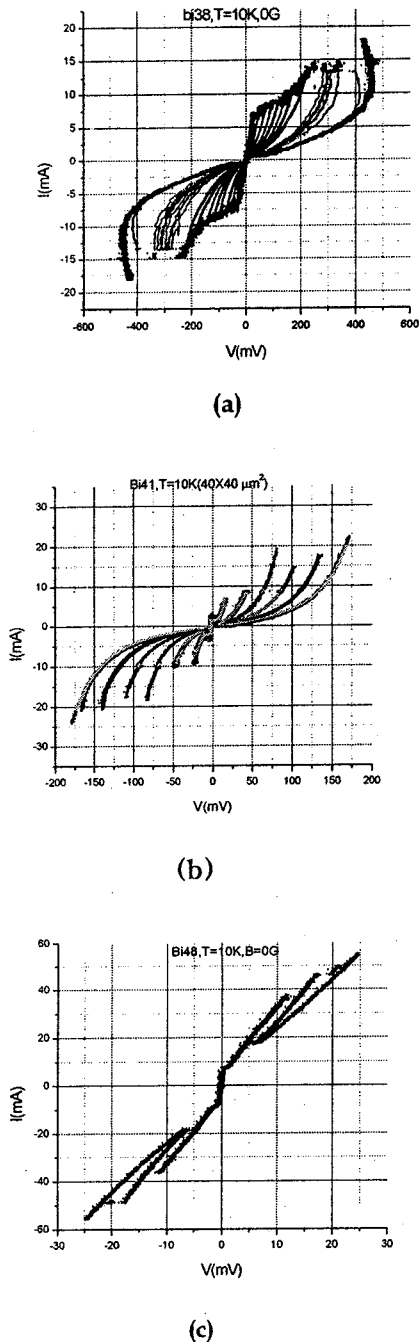


**FIG. 3.** I-V characteristics of different number of intrinsic junctions. The number of junctions are 20 in (a), 8 in (b) and 3 in (c).

Below  $T_c$ , I-V characteristics show a highly

hysteretic and multi-branched behavior as expected from a Josephson tunnel junction array with large capacitance.

The Stewart-McCumber parameter,

$$\beta_c = \frac{2\pi I_c R_n^2 C_J}{\Phi_0} \approx \left( \frac{4I_c}{\pi I_R} \right)^2 \quad (1)$$

(in the limit  $\beta_c \gg 1$ ), can be calculated using I-V characteristics of the first hysteretic branch.

Fig. 3 shows I-V characteristics of the samples with different number of intrinsic Josephson junctions. One can see multiple quasiparticle branches and it is in good agreement with the junction number estimated from the height of the mesa.

In fig. 3(a), we can observe negative dynamic conductance quasi-particle branches above 15 mA. This feature may occur due to the nonequilibrium heating which is caused by quasi-particle injection to the superconducting layers [7].

The McCumber parameter also varies as the number of junction decreases.  $\beta_c$  of junctions is 360 in the 20 layer stack, and 480 with 8 layer stack. For 8 layer stack with  $I_c \sim 2.7$  mA and  $R_n \sim 1 \Omega$ , we infer junction capacitance  $C_J \sim 57$  pF using eq. (1), which corresponds to  $\epsilon_J \sim 4.9$ . This value is consistent with the previously reported one [7]. Dynamic conductance ( $dI/dV$ ) of the resistive branch is almost infinite before jumping to the next branch. The voltage interval between these transitions can be regarded as the characteristic gap voltage, which is twice the superconducting energy gap,  $2\Delta/e$ , in an ideal SIS tunnel junction. Almost same values are obtained between the branches of the resistive state. In fig. 3, the gap voltage is 25 mV which is close to the energy gap of BSCCO probed by STM experiments [8]. This implies that the gap value obtained here is almost half of the superconducting energy gap. Yurgens *et al.*[9] suggested that this suppressed energy gap can be the result of the proximity-induced superconductivity in the BiO

layers.

### 3-2. Intrinsic Josephson junction in a parallel magnetic field

The DC intrinsic Josephson effect (IJE) was theoretically predicted only for small junctions with in-plane size  $L_{ab}$  smaller than  $\lambda_j$  ( $\sim 1\mu\text{m}$ ). In that case,  $I_c$  varies as a function of magnetic field and shows Fraunhofer behavior.

$$I_c(H) = I_c(0) \left| \frac{\sin(\pi s L H / \Phi_0)}{\sin(\pi s L H / \Phi_0)} \right| \quad (2)$$

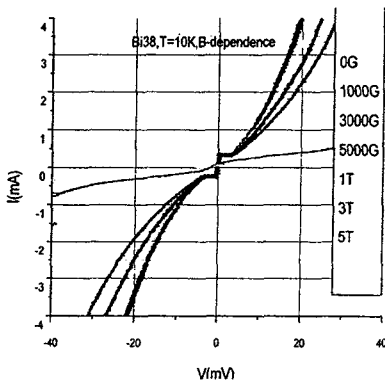
where  $\Phi_0$  is the flux quantum,  $L$  is the junction size perpendicular to  $H$ ,  $s$  is spatial periodicity of the stack.  $I_c(0)$  is the maximum Josephson current defined by the current density  $J_c(0)$

$$J_c(0) = c \Phi_0 / (8\pi^2 s \lambda_c^2), \quad (3)$$

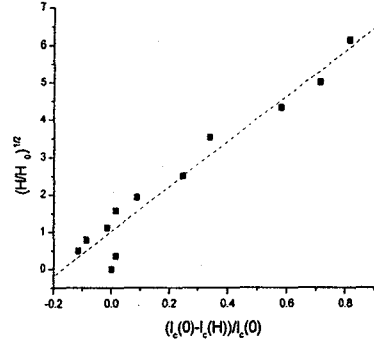
where  $\lambda_c$  is the c-axis London penetration depth. Using  $\lambda_{ab} = 0.3 \mu\text{m}$ ,  $s = 1.5 \text{ nm}$ ,  $v = \lambda_{ab} / \lambda_c \sim 1300$ ,  $J_c(0)$  is about  $1500 \text{ A/cm}^2$ .

In our data,  $J_c \sim 500 \text{ A/cm}^2$  is lower than the predicted one which may be due to the possible degradation of the superconducting property during the fabrication process.

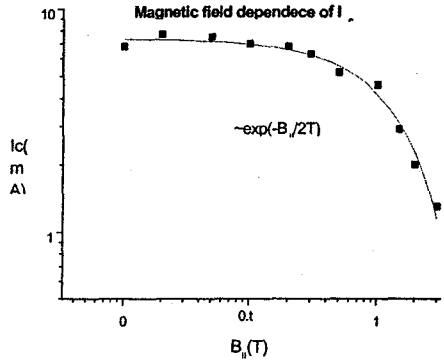
The first minimum of  $I_c(H)$  appears at  $H_1 = \Phi_0 / sL$  which is about  $300 \text{ G}$  for  $40 \mu\text{m}$  junction. Our samples are in the long-junction limit, that is,  $L \gg \lambda_j$ . So eq. (2) should be modified. Recent calculation predicts a universal, size independent decrease of  $I_c(H)$  [10].



(a)



(b)



(c)

FIG. 4. (a)Magnetic field dependence of IJJ with 20 layers. Critical current is chosen as  $I_{\text{max}}$  of first resistive branch.(b)Square root fit of  $I_c(H)$  (c)Exponential fit of  $I_c(H)$

$$\frac{I_c(0) - I_c(H)}{I_c(0)} \approx \sqrt{H/H_0}, \quad (4)$$

where  $H_0 = \Phi_0 \lambda_{ab} / \pi^2 s^2 \lambda_c$ , which is about  $700\text{-}800 \text{ G}$ .

Latsyshev *et al.* reported that oscillations in  $I_c(H)$  begin to appear in the junctions with size smaller than  $20 \mu\text{m}$  [2].

In fig. 4(b),  $I_c$  fits well to eq. (4). Also Yurgens *et al.*[4]. reported  $I_c(B)$  varies as  $\exp(-B/B_0)$  according to the pinned Josephson vortices model. This model assumed that the pancake vortices are caused by small misalignment between the magnetic field and ab planes of angle  $\theta$ . And these pancake

vortices are the main pinning centers for Josephson vortices. In fig. 4(c), the exponential fit is also in good agreement with our data.

### 3-3. AC intrinsic Josephson effect

For a short Josephson junction with  $L < \lambda_J$ , it is well known that constant voltage steps (Shapiro steps) appear in the I-V characteristics. In the array of Josephson junctions, it would be modified as:

$$V_m = Nm(\hbar/2e)\nu, \quad (5)$$

where  $\nu$  is the frequency of the applied electromagnetic (EM) wave and  $N$  is the number of the junctions, and  $m$  indicates the  $m$ -th step. For a long Josephson junction with  $L > \lambda_J$ , fluxons enter when we apply magnetic field, and they are driven by the current through the junction. This motion of the fluxon generates EM radiation with frequency  $\nu$  given by Josephson relation:

$$\nu = (2e/\hbar)V = cV/\Phi_0, \quad (6)$$

where  $V$  is DC voltage induced by the fluxon motion.

We would consider the flux-flow regime which is manifested by the flux-flow step in the I-V curve. In fig. 5 we can see additional branches in the I-V characteristics. These resistive branches are regarded as the flux-flow branches (FFB) caused by Josephson vortex flow in the intrinsic Josephson junctions because their spacing in the voltage,  $\Delta V$ , increases with increasing magnetic field.

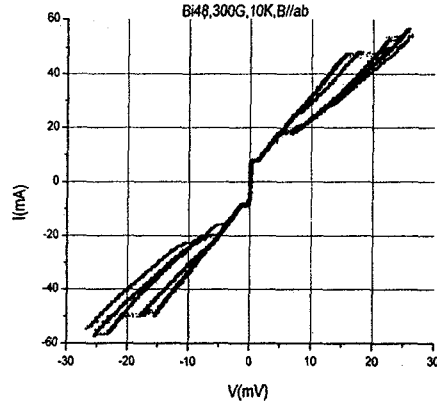
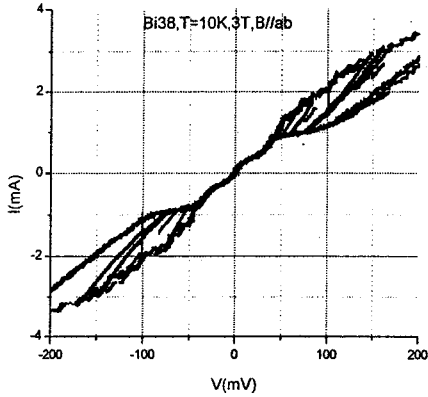


FIG. 5. IJJ with 3 layers in a magnetic field  $B=300$  G. Multiple flux flow branches are shown.

In the flux-flow state, fluxons are moving at a velocity  $v$  and the radiation frequency is given by  $\nu=v/\Lambda$ , where  $\Lambda$  is the spacing between the moving fluxons. A resonance occurs at the frequency where  $\nu$  is equal to the velocity of the EM wave ( $\bar{c} = cs/(\lambda_{ab}\sqrt{\epsilon_c})$  is the Swihart velocity) in the junction. Bulaevski *et al.*[11,12] proposed that in a high parallel magnetic field ( $H > H_0$ , where  $H_0$  is characteristic field,  $H_0 = \Phi_0/vs^2$ ), a triangular lattice of Josephson vortices should be formed. This triangular lattice is rigid enough to move as a whole when we drive a current across the layers. When the lattice velocity  $v$  is equal to  $\bar{c}/2$ , resonance occurs: and  $\epsilon_c$  is the dielectric constant between the conducting layers.



**FIG. 6.** IJ with 20 layers in high magnetic field  $B=3T$ . Flux flow step is observed at low current.

Fig. 6 shows I-V characteristics at  $H = 3 T$ , which is larger than the characteristic field of  $0.8 T$ . There is no branch up to characteristic voltage  $V_0$  and the step of low differential resistance appears below  $V_0$ . This step has no hysteresis, and this means all junctions are synchronized.

By combining the following equations

$$v = \bar{c}/2, \Lambda = \Phi_0/Hs, V = (v/c)(\Phi_0/\Lambda), \quad (7)$$

we get characteristic resonant peak voltage  $V_0$  as:

$$V_0 = \frac{1}{2} N \frac{\bar{c}}{c} sH, \quad (8)$$

where  $N$  is the number of the layers in which Josephson vortex moves. Fig. 7 shows the dependence of the maximum step voltage on the magnetic field.

At  $3 T$ , the value of  $V_0$  was estimated to be about  $40 mV$  using  $\lambda_{ab}=170 nm$ ,  $s=1.5 nm$ ,  $\epsilon_c=10$ ,  $\bar{c}/c=2.8 \times 10^{-3}$ , and  $N=20$ . This is close to the experimental value. Hence we concluded the observed step of low differential resistance is the flux-flow related step which is due to the collective motion of the Josephson vortex lattice.

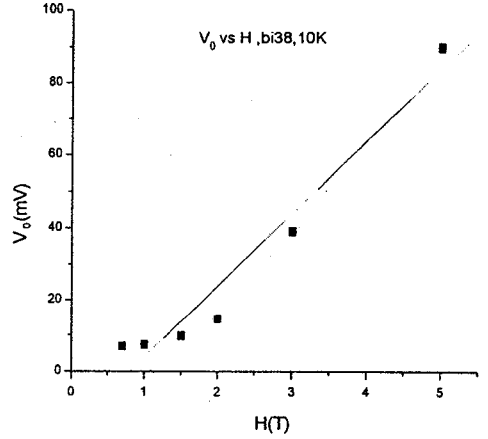


**FIG. 7.** Magnetic field dependence of maximum step voltage  $V_0$

Since the Swihart velocity is rather high, we can expect high frequency EM wave is generated at  $V=V_0$  with the frequency

$$\nu \approx \frac{\bar{c}sH}{2\Phi_0} \quad (9)$$

which is  $\nu=0.3 THz$  for  $H=1T$ .

This observation suggests that intrinsic Josephson junctions can be used as a high frequency local oscillator.

#### 4. Summary

We have measured c-axis transport property of BSCCO intrinsic Josephson junctions in a magnetic field parallel to ab planes. And we could control the height of the mesa within  $10 nm$ , and the samples contained only a few intrinsic junctions. In a magnetic field, we observed flux-flow branches in the I-V characteristics and found flux-flow step which indicates collective motion of the Josephson vortices. This observation shows the possibility of using intrinsic Josephson junctions as high frequency local oscillators.

#### 5. References

- [1] R. Kleiner, P. Muller, *Physica C* **293**, 156 (1997).
- [2] N. Kim, Y. Doh, H. Chang, and Hu-Jong Lee, *Phys. Rev. B* **59**, 14639 (1999).
- [3] Y. Latyshev, P. Monceau, V. Pavlenko, *Physica C* **293**, 174 (1997).
- [4] A. Yurgens, D. Winkler, T. Claeson, G. Yang et al, *Phys. Rev. B* **59**, 7196 (1999).
- [5] T. Yamashita, *Physica C* **293**, 31 (1997).
- [6] A. Yurgens, D. Winkler, T. Claeson, N. Zavaritsky, *Appl. Phys. Lett.* **70**, 1760 (1997).
- [7] A. Irie, Y. Hirai, and G. Oya, *Appl. Phys. Lett.* **72**, 2159 (1998).
- [8] J. Liu et al, *Phys. Rev. B* **49**, 6234 (1994).
- [9] A. Yurgens, D. Winkler, N. Zavaritsky, T. Claeson, *Phys. Rev. B* **53**, R8887 (1996).
- [10] M. Fistul, G. Giuliani, *Physica C* **230** (1994).
- [11] L. Bulaevskii, J. Clem, *Phys. Rev. B* **44** 1023419 (1991).
- [12] L. N. Bulaevskii, J. Clem, L. Glazman, *Phys. Rev. B* **46**, 350 (1992).